Acta of Bioengineering and Biomechanics
Vol. 24, No. 2, 2022

Original paper
DOI: 10.37190/ABB-02055-2022-02

Comparative analyses of blood flow through mechanical trileaflet and bileaflet aortic valves

MAREK PAWLIKOWSKI*, ANNA NIERODA

Warsaw University of Technology.

Purpose: The primary aim of the present study was to compare the bileaflet and trileaflet aortic valves' performance during uniform blood flow model and boundary conditions. The secondary aim of the study was to determine the effect of Newtonian/non-Newtonian fluid flow assumption on blood flow directly behind the trileaflet valve. *Methods*: The geometrical model of the whole system consist of the left ventricle, fragment of the aorta and mechanical valves. A representation of pulsatile flow was obtained by measuring blood flow velocity (Doppler ultrasound examination). We have assumed turbulent blood flow. We considered two blood models, Newtonian and non-Newtonian (Carreau model). The valves' performance was assessed using the reduced stress in the valves, the shear stress in the aortic wall, flow velocity field and the effective orifice area. *Results*: The maximum von Mises stress for the bileaflet valve leaflets was 0.3 MPa and for the trileaflet valve – 0.06 MPa. The maximum flow velocity for the bileaflet valve was 4.52 m/s for 40° and for the trileaflet valve – 5.74 m/s. Higher shear stress was present in the bileaflet (151.5 Pa) than for the trileaflet valve (49.64 Pa). *Conclusions*: The results indicate that central blood jet for the trileaflet valve contributes to more physiological blood flow and decreases the risk of haemolysis. The central flow minimises the risk of leaflet dislocation. In addition, lower stresses extend the durability of the valve. However, the trileaflet valve geometry has also disadvantages, for instance, small peripheral streams or relatively low effective orifice area.

Key words: *aortic valve, mechanical valve, blood flow, trileaflet valve*

1. Introduction

Artificial heart valves, often referred to as mechanical valves, have been implanted since the 1950s. Every year, around 300 000 artificial heart valves are clinically applied [10]. By the highest systemic loads, the most frequently replaced valve is the aortic valve.

The function of the aortic valve is to constantly regulate the blood flow. Any malfunction of the valve can lead to the creation of coagulated masses of blood, which flows through the cardiovascular system and can cause undesirable obstruction of vessels of small cross-sections. The bileaflet (BIL) mechanical aortic valve has been studied for years. Despite many studies, there is still a problem with thrombus formation, leading consequently to anticoagulation therapy, in patients with an implanted mechanical heart valve. It has been reported that an unphysiological fluid flow pattern determines thrombosis formation. Therefore, we started to work on designing a mechanical trileaflet heart valve that could correspond to the construction of the natural aortic valve and allow for central blood flow.

Recent numerical simulations of blood flow through mechanical valves have shown various approaches in modelling the haemodynamic effects. The haemodynamic consequences of blood flow across a mechanical valve were studied in silico with different flow patterns (laminar or turbulent), blood was defined as a Newtonian or non-Newtonian fluid, and various boundary conditions were assumed. In Table 1, the review of blood flow modelling through the bileaflet and trileaflet (TRI) mechanical aortic valves is briefly summarized.

* Corresponding author: Marek Pawlikowski, Institute of Mechanics and Printing, Warsaw University of Technology, ul. Narbutta 85, Warszawa 02-524, Poland. E-mail: marek.pawlikowski@pw.edu.pl

Received: March 15th, 2022
Accepted for publication: May 26th, 2022

Table 1. Summary of the literature review on modelling blood flow through BIL and TRI valves

Paper	Aim of study	Blood flow	Boundary conditions (BCs)
[19]	Structural strength comparison of two BMHVs	No blood flow	Fluid pressure applied on leaflet surface
[35]	Simulation of platelets around hinges during the mid-diastole phase	Laminar, Newtonian fluid	Flat level velocity BC and stress-free BC
[31]	Investigation of flow downstream of a dysfunctional BMHV	Turbulent, k-ω model, Newtonian fluid	Velocity flow BC (inlet), ambient pressure (outlet)
[1]	Numerical quantification of the implantation tilt angle of BIL on platelet activation	Laminar, Carreau–Yasuda model, Non-Newtonian fluid	The physiological blood velocity profile
[17]	Comparison hinge microflow fields of BIL	Turbulent, Spalart–Almaras model, Newtonian fluid	Velocity and pressure BCs were prescribed using the given waveforms
[16]	Pannus formation on blood flow through a bileaflet heart valve	Turbulent, Newtonian fluid	Physiological inflow rate
[14]	To elucidate the effect of coronary arteries in the leakage flow through hinges in BILs	Non-Newtonian fluid	Velocity BCs, Windkessel model at outlets
[21]	To develop a fully-coupled fluid-structure interaction framework that combines smoothed particle hydrodynamics and nonlinear finite element method to be applied in the investigation of the aortic and mitral valve's response	Smoothed particle hydrodynamics	Pressure profile
[3]	Investigation of nonlinear leaflet material properties influence on aortic valve dynamics	Turbulent, Newtonian fluid	Pressure profile
[5]	To determine the fluid and structural dynamics of aortic valves	Turbulent, Newtonian fluid	Zero-gradient pressure
[9]	Optimisation of the leaflet profile to obtain the lowest pressure gradient in forwarding flow, the lowest maximum velocity in the flow and the highest effective orifice area.	Turbulent, Newtonian fluid	Velocity flow BC (inlet), zero pressure (outlet)
[24]	Analysis of haemodynamic and thrombogenic properties	Newtonian fluid	Mie-Grüneisen equation of state relating pressure and internal energy per unit volume

There are relatively few reported studies of blood flow simulation through a trileaflet mechanical aorta valve. Bruecker and Li [7] introduced an *in vitro* pulse-duplicator generating early helical flow in the valve plane and experimentally investigated the influence of that flow on fluid behaviour after bi- and trileaflet valves in the ascending aorta. They hypothesised that physiological right-handed helix in the ascending aorta might partly be maintained by early swirl in the ventricle outflow tract entering the aortic arch. They concluded that the TRI valve better conserved the helical flow than the BIL valve. Schaller et al. [28] implanted four novel mechanical prostheses of the aortic valve in sheep. The mechanical valves consisted of three leaflets made of poly-ether-ether-ketone. The housing was manufactured from medical-grade titanium-aluminium-vanadium alloy (TiAl6V4). The *in vivo* preliminary results were auspicious because the valves induced excellent haemodynamic and are characterised by a shallow risk of thrombotic events.

The primary aim of the present study was to compare the BIL and TRI aortic valves' performance during uniform blood flow model and boundary conditions. To complete the task, we performed numerical simulations of the flow through the TRI valve. The review of the literature shows that the blood flow simulations conducted under various assumptions. The available comparative studies pertaining BILs and TRIs show superiority of TRI valves over BILs [13], [18]. In the cited research, however, the authors simulated blood as a Newtonian fluid and investigated a polymeric TRI valve [13] or a metallic one with thin leaflets [18]. Our research followed that conclusion and introduced a design of a TRI valve and compared its haemodynamic performance to a BIL valve. The results of the simulations may contribute to the determination of new design parameters for trileaflet aortic valves, which can improve their cardiologic performance and ensure proper haemodynamic parameters. The TRI design presented in the paper is the first conceptual approach that we wanted to verify.

The secondary aim of our study was to determine the effect of Newtonian/non-Newtonian fluid flow assumption on blood flow directly behind the trileaflet valve, as that concerning the bileaflet valve is very well known [6].

In the paper, 3D flow patterns and velocity profiles of blood flow in the aorta behind the two types of mechanical valves are presented. Achieving more real behaviour of blood stream during cardiac cycling is possible by including the ventricle in the numerical model.

2. Materials and methods

Study design

The main objective of this study was to analyse the flow through the TRI and BIL mechanical aortic valves. A pulsatile flow image, obtained by measuring blood flow velocity (Doppler ultrasound), was applied to define the boundary conditions. Navier–Stokes equations were used to define the flow.

Two different numerical methods are widely used in the study of flow through heart valves. One approach neglects the leaflet motion, focusing on fixed leaflets with constant or pulsatile flow [30], [34]. The other method is to simulate the movement of the leaflets. In our research, we decided to analyse the blood flow at three positions of the valves' leaflets defined using angle with respect to the vertical plane (passing through the symmetry axis of the valve) 40°, 20° and 0° (fully opened valve). A scheme of the complete opening of the valve is shown in Fig. 1.

The pulsatile nature of the blood and the geometry of the natural system means that vortices can form behind the aortic valve. To reflect physiological flow as accurately as possible, we have assumed turbulent blood flow and utilized the k-ε model to define its turbulent characteristics.

In our work, we investigated the shear effect for which the fluid model adopted can be of great importance. We, therefore, considered two blood models (Newtonian and non-Newtonian) during blood flow through the TRI valve. There is still a general opinion that blood can be modelled as Newtonian in the case of large arteries, so, based on the results, we determined how the adopted blood model affects the results. Blood flow through the BIL valve was modelled as non-Newtonian.

By defining blood as incompressible Newtonian fluid we assumed the density ρ = 1060 kg/m^3 and viscosity μ = 0.0035 kg/(m·s) [2]. For the non-Newtonian blood flow, we defined the Carreau model. We have assumed the following parametric values: relaxation time constant λ = 3.313 s, zero shear rate limit μ_0 = 0.056 Pa·s, infinite shear rate limit μ_∞ = 0.0035 Pa·s and power low index n = 0.3568 [29].

The ventricle and aorta materials were assumed to be isotropic and elastic medium with the Young modulus E_a = 1 MPa and Poisson's ratio v = 0.49. The leaflets were also modelled as an isotropic elastic solid material with the Young modulus E_l = 2884 MPa, v_l = 0.39, and the ring material was modelled as titanium alloy Ti-6Al-4V, whose characteristic mechanical parameters are: $E_r = 1.07 \cdot 10^5$ MPa, v_r = 0.3.

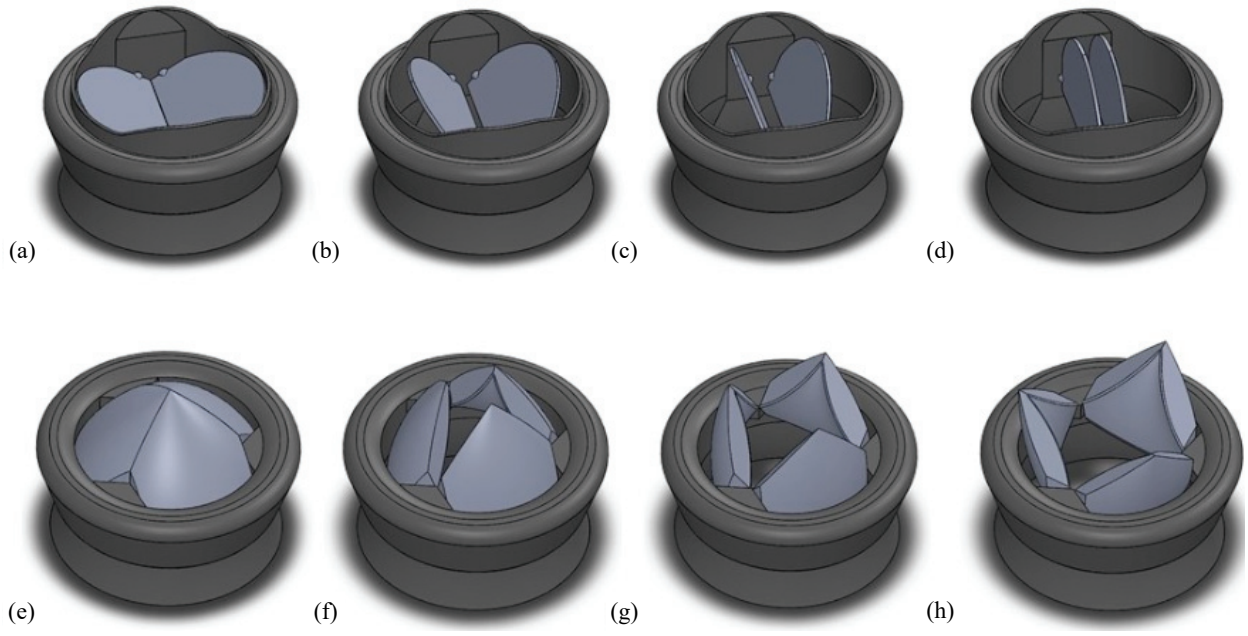

Fig. 1. Analysed leaflet positions for the BIL valve: a) 60°, b) 40°, c) 20°, d) 0° and for the TRI valve: e) 60°, f) 40°, g) 20°, h) 0°

Geometrical modelling

The geometrical model of the whole system consisted of the left ventricle and a fragment of the aorta. The model was based on the data available on the GrabCAD platform (https://grab cad.com/). The geometric model simplifies the cardiac and aortic anatomy, but the defined values of the model parameters are consistent with reality. We used SolidWorks 2019 CAD software to create the 3D models of the anatomical components of our system and those of the valves (Fig. 2).

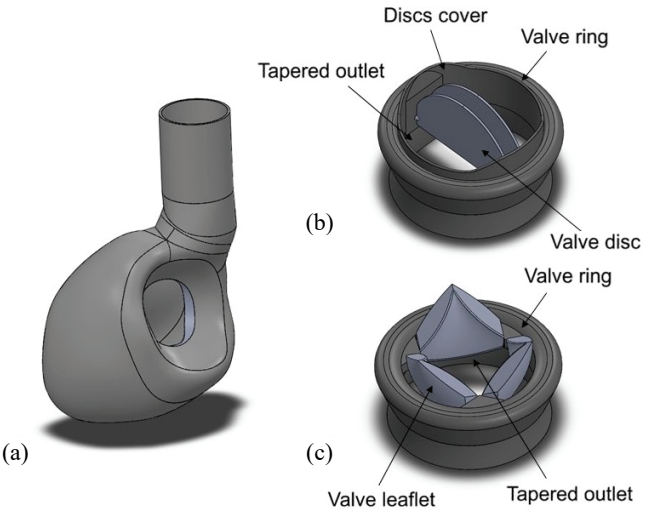

Fig. 2. Solid model of the: a) left ventricle and fragment of the aorta, b) BIL valve, c) TRI valve

In our study, we considered two types of mechanical valves, i.e., bileaflet valve and trileaflet valve. It has to be noted that although the models are based on the known designs of bi-and trileaflet valves, our models of the valves differ from them mainly in the construction of the annular ring. The internal diameter of the outlet of both prostheses is 21 mm, the external diameter of the ring is 27 mm, the profile height is 16.5 mm. Additional, for the TRI valve, we proposed a new leaflet curvature (Fig. 3). The shape of the leaflets influences the pattern of velocity fields which determine the haemodynamic quality of the valve. The valve outlet surface is tapered. In the presented model of a BIL valve, the ring has additional covers to protect the leaflets in the closed position. The leaflets of both valves are embedded in blind holes, allowing them to rotate freely between 0° (fully open) and 60° (fully closed). In the open position, the plane of the leaflets of a BIL valve forms an angle of 90° to the surface of the outlet. The presented models are simplified. In fact, the ring's rim is lined with material, attached through titanium fastening rings, which enables the valve to be implanted in the outlet of the aorta.

The internal diameter of the ascending aorta was assumed to be 27 mm and its length 40 mm.

Mesh quality

The mechanical model mesh was made of 150 000 finite elements. The mesh densification was

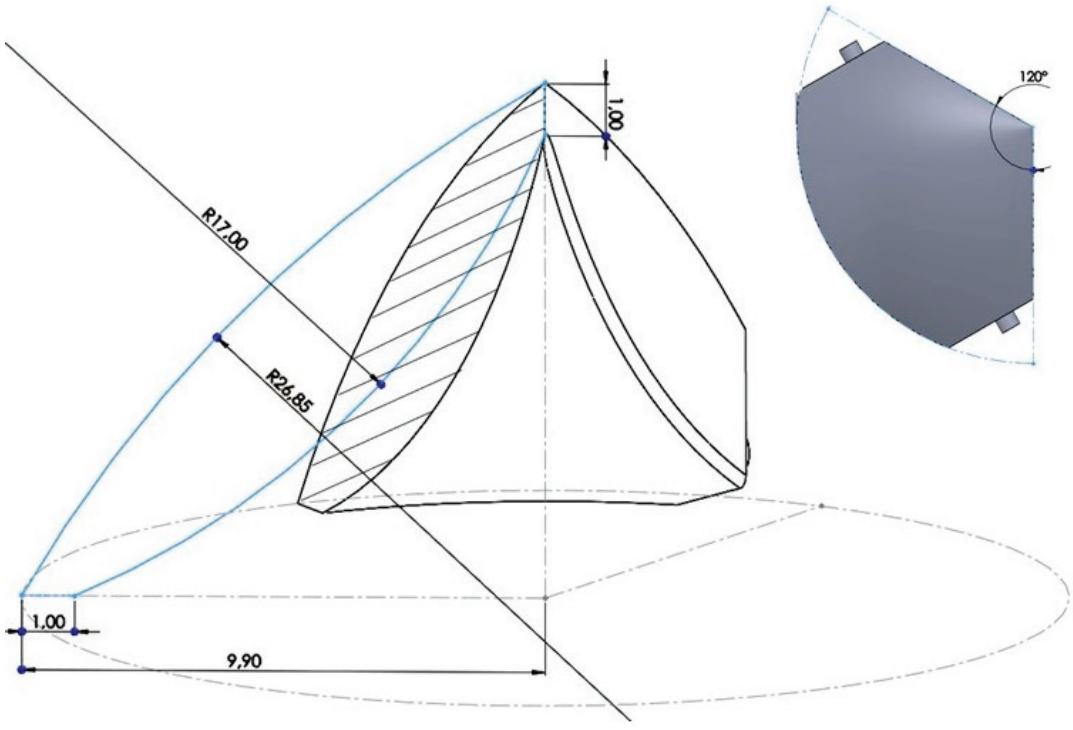

Fig. 3. Shape of the TRI valve leaflet

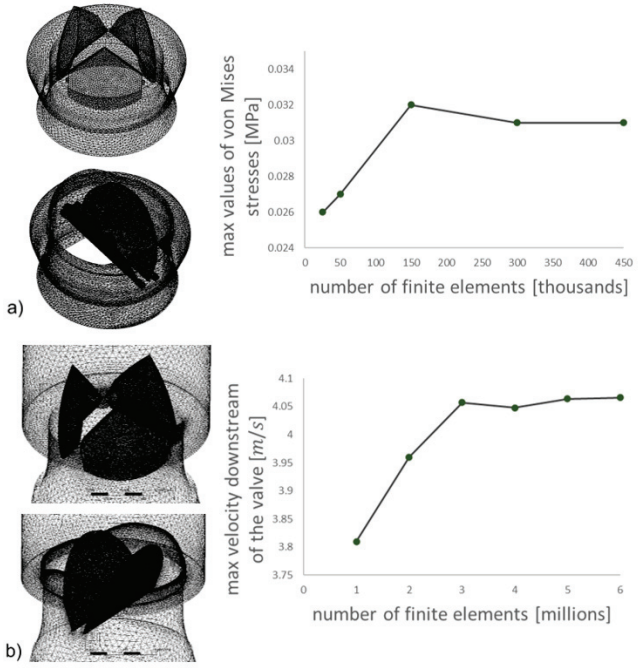

Fig. 4. Influence of the number of the finite elements on (a) maximal von Mises stress values in TRI valve leaflets and (b) maximal velocity downstream of the TRI valve

performed for the valve leaflets, valve ring and ascending aorta (these areas participated in the FSI analysis). We confirmed the mesh independence of the mechanical model solution by comparing the reduced stress values on the valve leaflets in FSI conditions (Fig. 4a). We have verified that the number of the finite elements, which define our model, higher than the mentioned value 150000 influence the results, i.e., values of stress, by approx. 1%. The solid imitating blood was created with 3 million finite elements. We verified the mesh independence of the flow model solution conducted under steady-state flow by comparing the max velocities downstream of the valve (Fig. 4b). In addition, the quality of the mesh representing blood was checked. The Orthogonal Quality was about 0.8, and the Skewness was about 0.22. The values obtained indicate a grid of good quality.

Boundary conditions

The representation of pulsatile flow was obtained from literature data [4], [22], [33]. The authors received blood velocity measurements during their study, on which the below assumptions were based. The correlation of the flow velocity and the time opening of the leaflets was determined utilising the Doppler ultrasound examination in an adult human being [4]. A 6th-degree polynomial interpolation (Eq. (1)) was used to describe the flow mathematically. In the time span from 0.36 s to 0.38 s a linear function was adopted (Eq. (2)). The flow velocity at the time that followed until the end of the cycle was described using Eq. (3). The length of one cycle was assumed to be 0.8 s. Heart rate was 75 beats per minute.

for $t \in \langle 0;\ 0.36\ \text{s}\rangle$

$$v = 10269.13t^6 - 13602.92t^5 + 6827.23t^4 - 1500.76t^3 + 90.61t^2 + 9.54t, \tag{1}$$

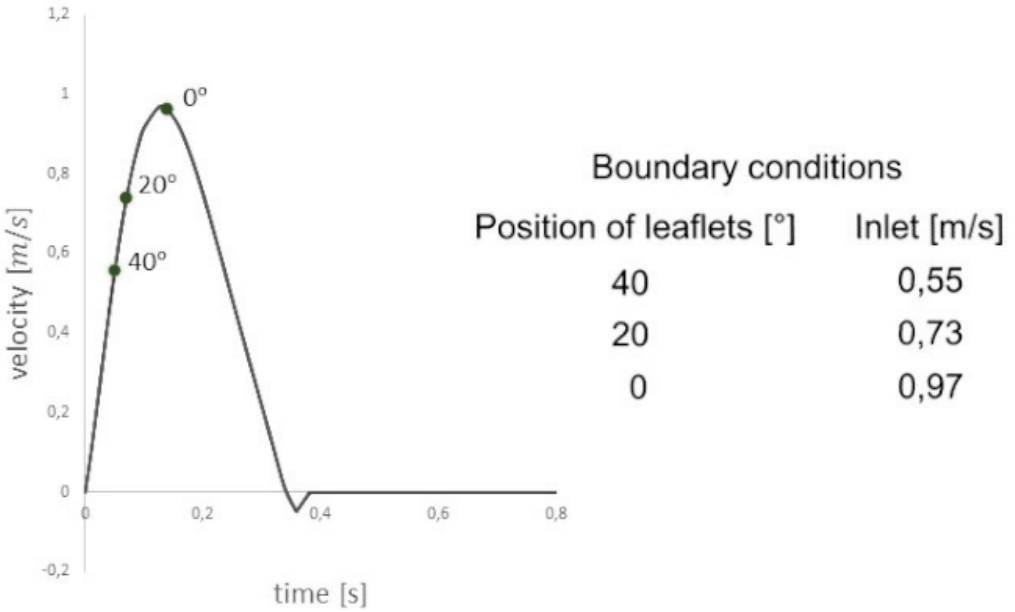

Fig. 5. Boundary conditions

for $t \in \langle 0.36; 0.38\ \mathrm{s})$

$$v = 2.5t - 0.95\,, \tag{2}$$

for $t \in \langle 0.38; 0.8\ \mathrm{s})$

$$v = 0. \tag{3}$$

It was assumed that the valve opens at 0.04 s of the flow cycle, and the process of the valve opening lasts 0.04 s [11]. The valves are, thus, fully opened after 0.08 s of the flow cycle. Regarding this, the values of the flow velocity at the considered leaflet positions were estimated utilising Eq. (1).

The flow velocity values were determined at the inlet, which was defined at the entrance to the left ventricle. A constant pressure of 14 kPa was described at the aortic outlet, corresponding to the average pressure of the systolic and diastolic phases in a healthy human [26]. Boundary conditions are summarised in Fig. 5.

Numerical modelling of blood flow

The dynamics of blood circulation were determined using ANSYS 2020 R2 software. Three modules for blood flow analysis were used. The Mechanical module allowed us to determine the stress in the valve as well as in soft tissues. The Fluent module was used to define the flow parameters. The System Coupling module provided data exchange. We used Two-Way Coupling Methods. Such a solution made it possible to perform FSI analyses, which made it possible to determine the precise flow characteristics and the influence of structural response on cyclic fluid movement.

To determine the stress distribution across the entire system, the leaflet rotation constraints and the contact between the leaflet guiding elements and blind holes were defined. We used the "Frictional" model. The friction coefficient was assumed to be equal to 0.1. Frictional contact means that two contacting geometries can transmit shear stresses up to a specific value before they start sliding against each other.

A pressure-based solver was used for the calculations. Each data exchange step was recalculated five times (in the System Coupling module), preventing sudden stress value jumps and solver errors. The information exchange between solvers was done every 0.01 [s]. The number of steps was 20. The selection of a good

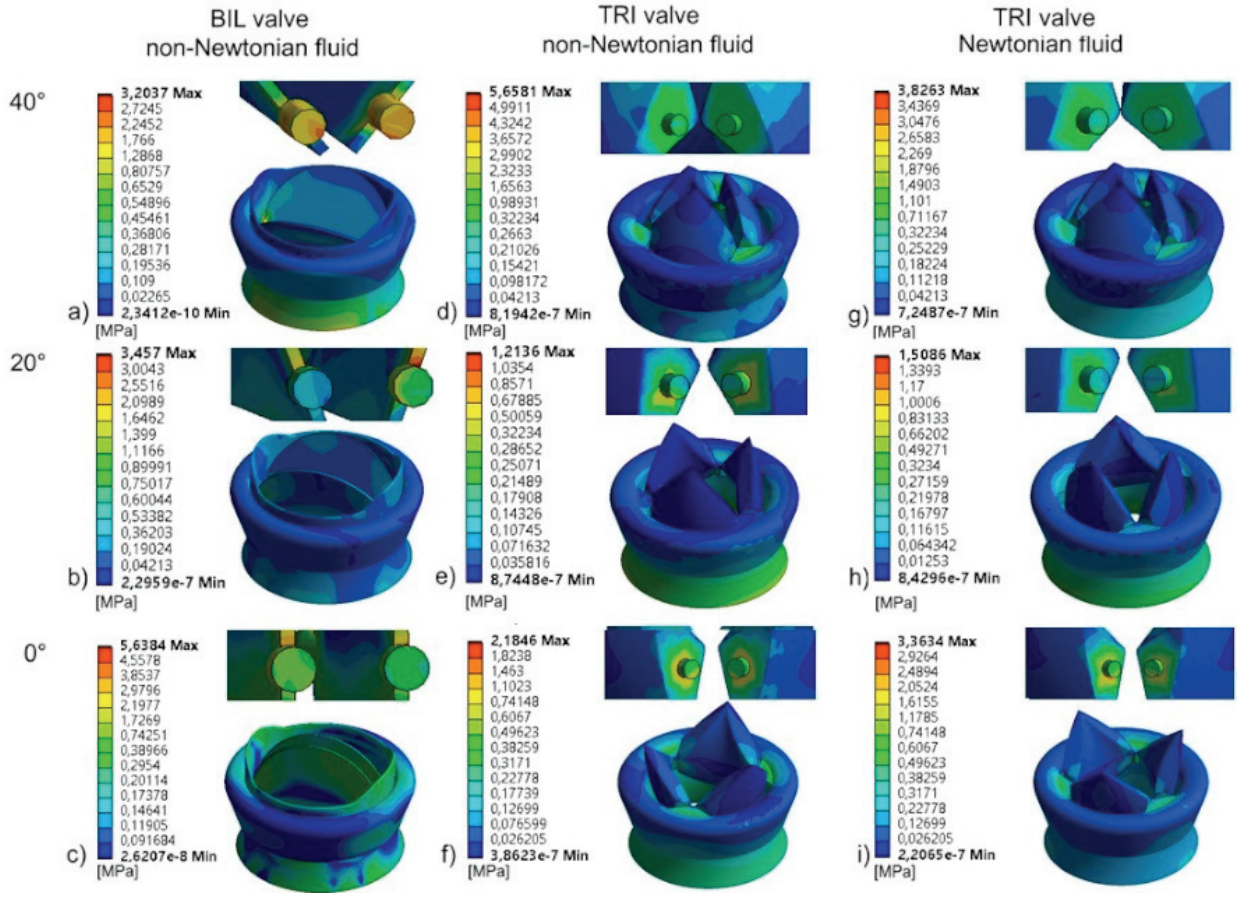

Fig. 6. Stress distributions in the valve for the BIL valve leaflets' positions: a) 40°, b) 20°, c) 0° and for the TRI valve leaflets' positions: non-Newtonian fluid d) 40°, e) 20°, f) 0°, Newtonian fluid g) 40°, h) 20°, i) 0°

quality mesh and a time step allowed for stable computations. Too large time step can affect the inaccuracy of the calculation, and too small time step is computationally expensive.

Simulations were performed on a workstation with the following parameters: AMD Ryzen 7 3700X 8-Core Processor, 32GB RAM, 64-bit operation system, and NVIDIA Quadro graphic card.

3. Results

In Figure 6, the stress distributions in the BIL and TRI valve leaflets in the positions considered are shown. The mounting of the leaflets in the valve ring was also analysed. These stresses are a consequence of the interaction of flowing blood with the leaflets. The results of the study are summarised in Table 2. In Figure 7, the flow of blood in the aorta for the same leaflets' positions is depicted.

Table 2. Maximum values of von Mises stress in the valves for the BIL and TRI (non-Newtonian and Newtonian fluid) valves

BIL valve non-Newtonian fluid			
Leaflet position [°]	Stress in the pivots [MPa]	Stresses in the ring [MPa]	Stresses in the centre of the disc [MPa]
0	5.09	5.64	0.30
20	2.94	3.46	0.20
40	3.02	3.20	0.17
TRI valve non-Newtonian fluid			
Leaflet position [°]	Stress in the pivots [MPa]	Stresses in the ring [MPa]	Stresses in the centre of the disc [MPa]
0	1.51	2.18	0.06
20	0.63	1.21	0.02
40	2.31	5.66	0.05
BIL valve Newtonian fluid			
Leaflet position [°]	Stress in the pivots [MPa]	Stresses in the ring [MPa]	Stresses in the centre of the disc [MPa]
0	2.99	3.36	0.08
20	0.82	1.51	0.02
40	1.62	3.83	0.07

In addition, the flow velocity field was shown in Fig. 8 to verify the symmetry of the flow.

In Figure 9, shear stress in the ascending aorta wall induced by the flow in the considered positions of the leaflets, i.e., 0°, 20° and 40°, is shown.

To evaluate the performance of the two types of mechanical valves, we also calculated the effective orifice area E_{OA}, representing the cross-sectional area of the jet issuing from the valve at the point of its most significant contraction. We used the corrected Gorlin formula in the form of [15]:

$$E_{OA} = \frac{Q}{51.6\sqrt{\frac{\Delta p}{\rho}}}, \tag{4}$$

where: Q is the root mean square of forwarding flow [mL/s], Δp is the mean pressure difference across the valve [mmHg], and ρ is the density of blood [g/cm^3]. The number 51.6 is the gravitational acceleration constant. We assumed the blood density to be 1.06 g/cm^3. The mean pressure difference Δp, as well as the blood flow, were calculated in the numerical simulations of blood flow.

The maximum effective orifice area is 1.53 cm^2 for a BIL valve for an opening angle 0° and for a TRI valve 0.49 cm^2 (opening angle – 20°).

4. Discussion

In the paper, we proposed our design of the mechanical TRI valve, which differs from those already presented in the literature by the shape of the leaflets (Fig. 3). Usually, authors offer a design with thin leaflets which, in the closed position, form a dome-like construction [20]. The inner curvature of the leaflets is an additional factor contributing to vortex formation in the blood flow. In addition, due to the light construction of the leaflets, they violently decelerate at the valve closure, which causes haemolysis by squeezing the blood cells. The available in silico, *ex vivo* [28], and *in vivo* modelling approaches provide an understanding of the diseases involved and help clinicians to predict the patients' reaction to the implanted valve. The *in silico* method we used allows one to avoid medical interference, e.g., transoesophageal echocardiography [27], which is troublesome to the patients and may result in medical complications.

Our numerical results seem to indicate that the proposed leaflets curvature in the TRI valve causes less turbulent blood flow. This is due to the streamlined shape of the leaflet (Fig. 3). This is manifested by the occurrence of smaller vortices behind the valve (Figs. 7d, e). This is highly desirable as turbulent flow is one of the factors leading to haemolysis reaction.

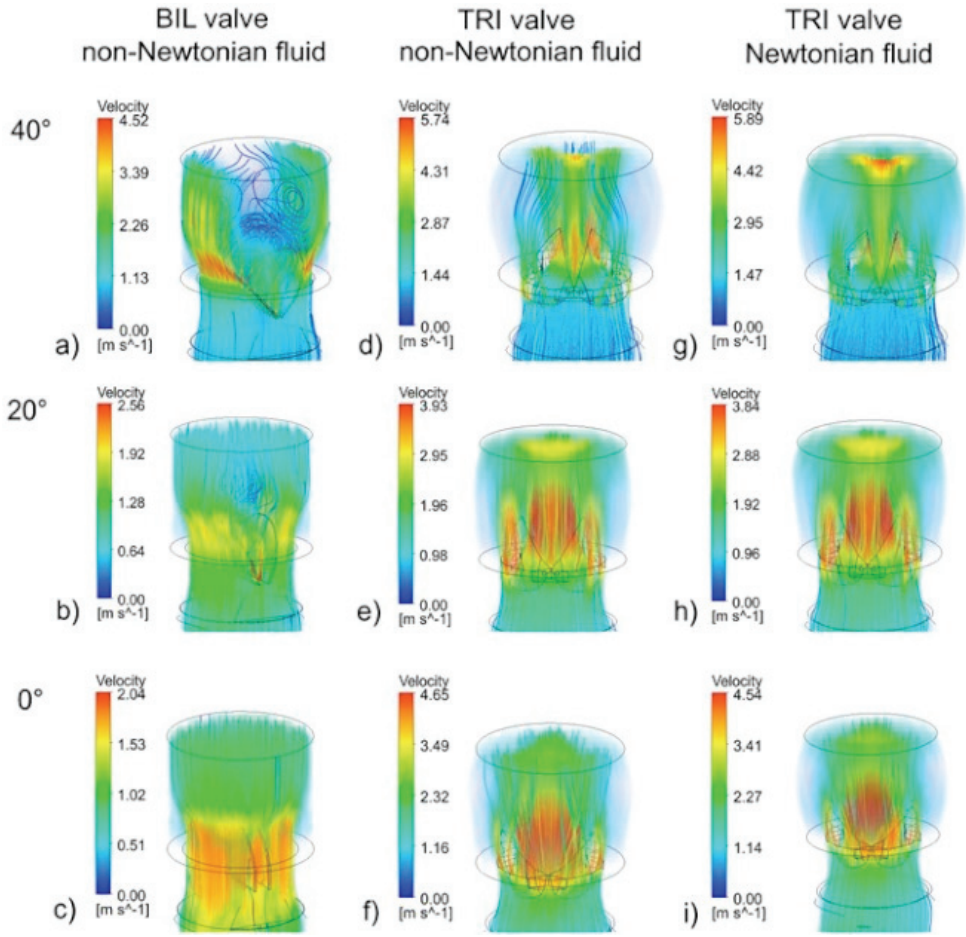

Fig. 7. Velocity fields of the flow through the BIL valve leaflets' positions: a) 40°, b) 20°, c) 0°
and for the TRI valve leaflets' positions: non-Newtonian fluid d) 40°, e) 20°, f) 0°, Newtonian fluid g) 40°, h) 20°, i) 0°

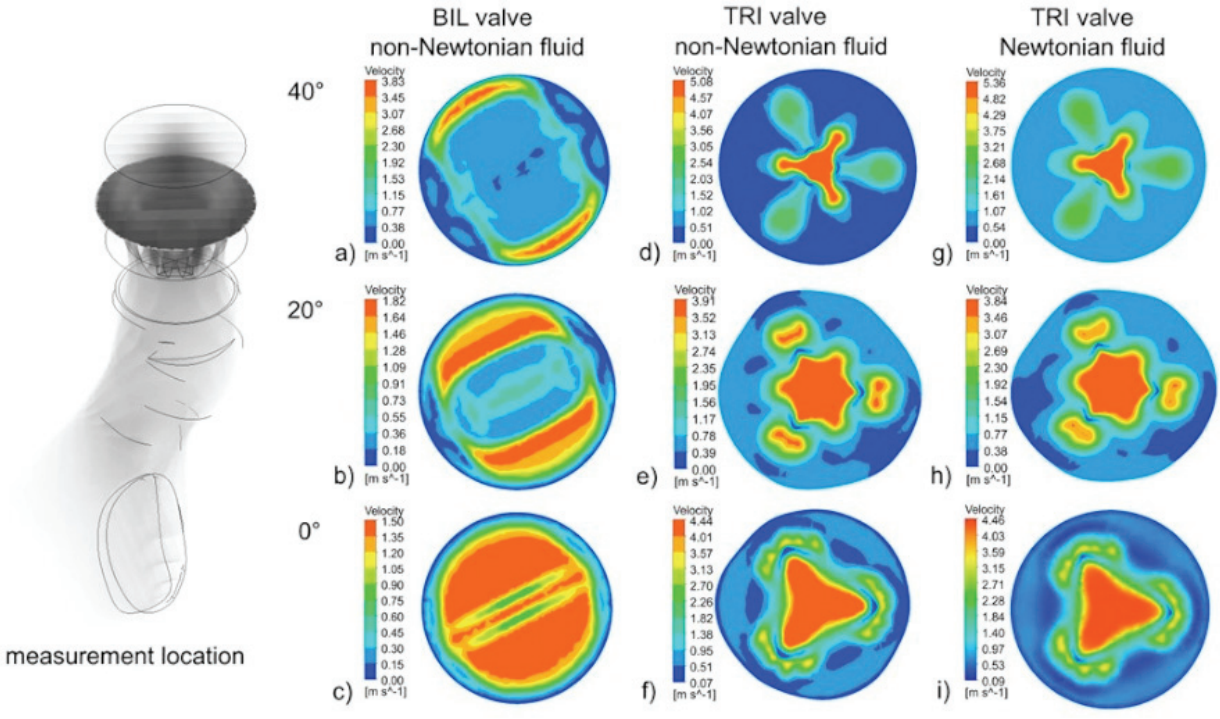

Fig. 8. Cross-sectional velocity fields for the opening angle of the BIL valve: a) 40°, b) 20°, c) 0°,
for TRI valve: non-Newtonian fluid d) 40°, e) 20°, f) 0°, Newtonian fluid g) 40°, h) 20°, i) 0°

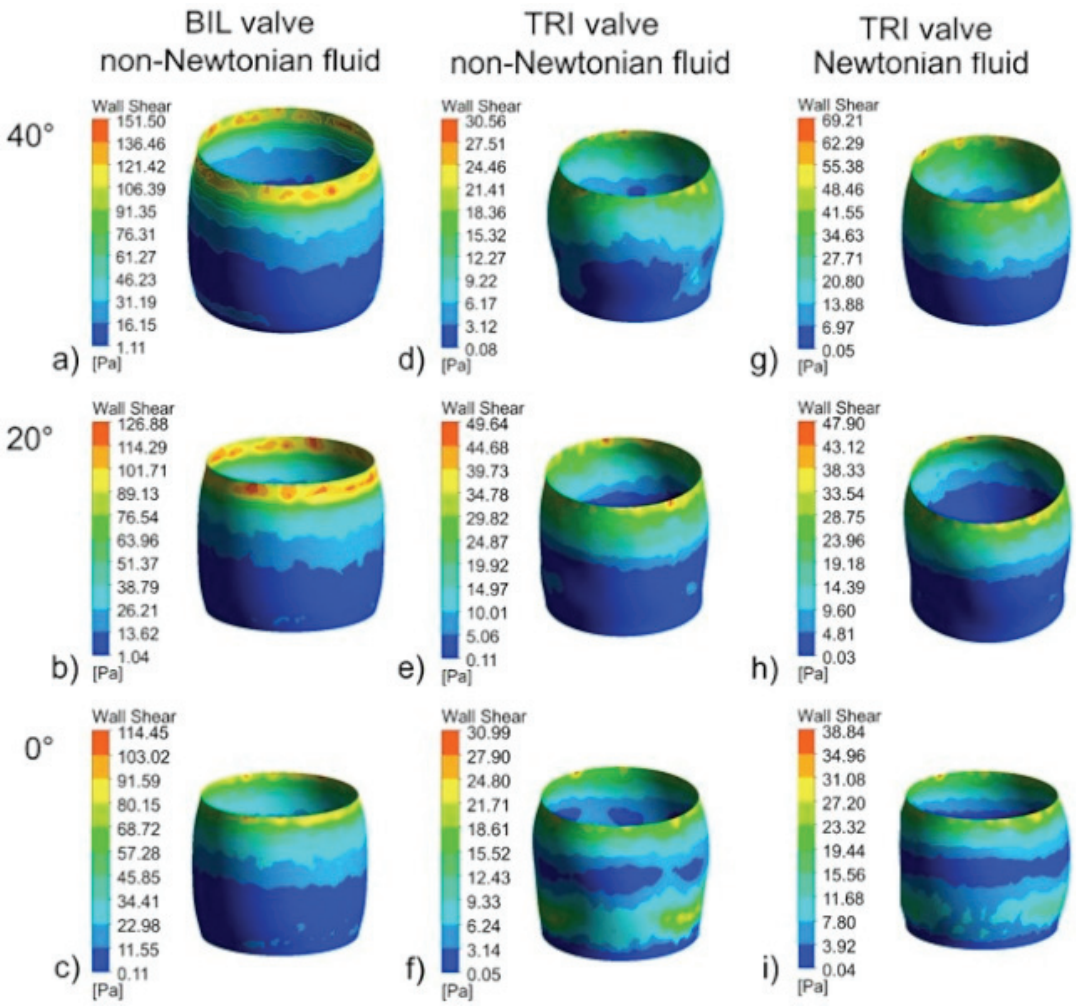

Fig. 9. Shear stress distributions in the ascending aorta wall for the BIL valve: a) 40°, b) 20°, c) 0°, for TRI valve: non-Newtonian fluid d) 40°, e) 20°, f) 0°, Newtonian fluid g) 40°, h) 20°, i) 0°

The vortices in the BIL valve during flow can be seen in Figs. 7a, b.

There is a common belief that in large vessels, blood can be modelled as a Newtonian fluid [16], [17], [31], [35]. However, such an assumption might be a too far-fetched simplification in certain situations, e.g., during a flow through a mechanical aortic valve. The blood flow through both BIL and TRI valves is highly inhomogeneous in space and time. Although the quantitative results of haemolysis simulations can differ with a non-Newtonian model applied, such an approach seems to give a more realistic wall shear stress distribution than a Newtonian fluid model [14].

Modelling blood flow through blood vessels, which form a branching structure, requires that the model of this structure must be truncated. In our studies, we defined a combination of flow rate and pressure at the inlet and outlet, respectively. This approach in modelling of the blood flow boundary conditions is commonly used [17], [31]. The choice of the defined boundary conditions is confirmed by obtaining blood flow velocity field values through the partially and fully open BIL valve (Figs. 7b, c) corresponding to values for the natural trileaflet aortic valve [32]. The instantaneous maximum velocity for the BIL valve corresponds to the moment of valve opening (Fig. 7a). Compared to the BIL valve, there are significantly higher velocities in the TRI valve (maximum velocity value for BIL: 4.52 m/s, for TRI 5.74 m/s – non-Newtonian fluid and for TRI 5.89 m/s – Newtonian fluid). This is due to the curved shape of the TRI valve leaflets, which significantly affects the reduced flow field. Higher values of the flow velocity field for the case of a TRI valve compared to a BIL valve were also observed by Piatti et al. [24]. The velocity values for the Newtonian and non-Newtonian models are similar. However, the character of flow seems to be different for non-Newtonian and Newtonian fluid (Figs. 7d–f, g–i). We have used streamline techniques to visualize the flow and, in particular, its direction to make the analysis results more clear. The streamlines in Figure

7d–f show more clearly the peripheral flow than those in Fig. 7g–i. TRI valve flow shows deceleration of the peripheral flow for non-Newtonian fluid during leaflet opening (Fig. 7d). This reduction in flow velocity can have a negative effect on blood haemodynamics as it can lead to flow stagnation or cause haemolysis.

One of the very significant parameters influencing the behaviour of blood cells during flow is shear stress. According to Ge et al. [12], shear stress must be above 150 [Pa] to cause haemolysis and above 10 [Pa] to cause platelet activation. A high value of shear stress in the ascending aorta for the BIL valve (i.e., 151.5, 126.88 and 114.45 Pa for cusp position of 40, 20 and 0°, respectively) may indicate the possibility of haemolysis. The risk is high, but the duration of exposition would still need to be considered. Exceptionally high shear stress (151.5 Pa) occurs at the valve opening (40° – Fig. 9a). This stress is because the flow runs close to the aortic wall (Figs. 7a, 8a). Furthermore, vortices occur during valve opening (Figs. 7a, b), which further increases the impact of blood on the aortic wall. In the case of the BIL valve, a decrease of wall shear stress with the deceleration of flow can be noticed (compare Figs. 7a–c and Figs. 9a–c). This is due to the fact that the shear rate increases because the main streamlines of the flow are concentrated in the peripheral regions of the aorta, i.e., near the aorta wall, which drastically changes the geometry of the flow. As the blood is a shear-thinning fluid, which means that its viscosity decreases with a shear rate increase, a higher shear rate makes the blood less viscous, which causes lower wall shear stress. The wall shear stress for the TRI valve is much lower, i.e., 30.56, 49.64 and 30.99 Pa for leaflet position of 40, 20 and 0°, respectively (non-Newtonian fluid) and 69.21, 47.90 and 38.84 Pa for leaflet position of 40, 20 and 0°, respectively (Newtonian fluid) (Fig. 9). This is related to the central flow of blood (Figs. 7, 8). Due to the more established flow and decreasing flow velocity field, haemolysis should also not occur further down the aorta. The highest shear stresses in the TRI valve occur at an opening angle of 20° (Fig. 9e). Blood, in this case, flows through the gaps between the leaflets and the valve ring that form when the leaflet opens. Analysis of Figs. 9g–i shows that for Newtonian fluid, the maximal wall shear stress occurs at the angle of 40°, i.e., at the beginning of the valve opening. This is in accordance with Fig. 8g, which presents velocity distribution at the same leaflet position. The viscosity of a Newtonian fluid is constant, and the shear effects take place right after the beginning of the flow. In the case of non-Newtonian fluid, the viscosity changes with time. Therefore, we can observe the maximal wall shear stress at the mid-position of the leaflets (Fig. 9e) when the flow rate is low.

The allowable stress value for the valve design is 32 MPa [23]. The von Mises stress analysis indicates that the highest stresses occur at the hinges and the place of leaflet attachment (Table 2, Fig. 6). The moment of occurrence of the highest stresses, 0° for the BIL valve (5.64 MPa) and 40° for the TRI (5.66 MPa), is due to the highest velocity values near the hinges (Figs. 8c, d). The low stress values in the centre of the TRI valve leaflets (0.02–0.08 MPa) are influenced by the adopted thickness of the leaflets. According to Fig. 3, the TRI leaflets thickness value varies from 0.6 to 2.6 mm. For the BIL valve (leaflet thickness 0.4 mm), these values are in the range of 0.17–0.30 MPa. In Figure 8, the central flow at the TRI valve is directly shown. The results of our simulations indicate that the maximum stress values are much smaller than the allowable values. We, therefore, conclude that the construction of the valves will not fail. However, it should be noted that we considered 75 beats per minute. With an increase in heart rate, Nasif et al. [23] observed a significant increase in stress. Stress values we obtained may be underestimated due to the lack of consideration of recirculating flow. Exceeding the allowable stresses can lead to malfunction and failure of the valve over a long period, so valve motion analysis, which will be performed in future research, is necessary. BIL valve flow is symmetrical (Figs. 8a–c). It can, therefore, be concluded that the discs should not dislocate.

To better assess valve performance, clinicians have developed a E_{OA} parameter. The highest E_{OA} for the TRI valve corresponds to a valve opening angle of 20°. This is because the flow area at this position is the largest (170 mm^2). The effective orifice area for the trileaflet valve indicates that the valve leaflets are too thick. The correct area should be approximately 1.5 mm^2. Changing the curvature of the leaflet increases the flow area and reduces the flow velocity field value. This has positive effect on decreasing the pressure gradient upstream and downstream of the valve.

It is acknowledged that a TRI valve geometry causes more physiological closing compared to a bileaflet valve [8]. The rate of the leaflets closing influences the stimulation of platelet activation. Moreover, slower closing velocity decreases cavitation intensity [25] – another phenomenon contributing to blood cells deterioration. According to [8], the minimization of cavitation is also affected by thicker leaflets and a small rotation radius. Cavitation and valve motion will be the subject of our next research.

5. Conclusions

Although the design of our TRI valve is preliminary and needs to be optimised, our results highlight some advances of such a valve geometry. This is manifested mainly by a central blood jet, contributing to more physiological blood flow and decreasing the risk of haemolysis (maximum shear stress for the BIL valve is 151.5 Pa, for the TRI valve – 49.64 Pa] and, therefore, avoiding anticoagulation therapy in transplant patients. This will increase the possibility of implanting mechanical aortic valves in more patients. The central flow minimises the risk of leaflet dislocation. In addition, lower stresses extend the durability of the valve (maximum von Mises stress for BIL valve leaflets is 0.3 MPa and for the TRI valve – 0.06 MPa). Another feature of the TRI valve is that it ensures similar blood flow regardless of the implantation angle. This is not the case for the BIL valve, which causes different flow patterns under various implantation angular orientations. Our numerical results indicate that the proposed leaflet curvature in the TRI valve results in less turbulent blood flow. This is a positive aspect of the TRI valve leaflet design, as vortices increase the risk of haemolysis.

The analyses also point out to construction elements that should be improved. For instance, the parameter EOA should be increased. Reducing the curvature of the leaflet will increase the flow area and reduce the flow velocity field value. This will have a positive effect on decreasing the pressure gradient upstream and downstream of the valve.

The analyses confirm the validity of using three leaflets in constructing the TRI valve and indicate the advisability of further optimisation of the construction.

References

[1] ABBAS S.S., NASIF M.S., AL-WAKED R., SAID M.A.M., *Numerical investigation on the effect of bileaflet mechanical heart valve's implantation tilting angle and aortic root geometry on intermittent regurgitation and platelet activation*, Artif. Organs, 2020, 44 (2), E20–E39.

[2] ALI A., KAZMI R., *High performance simulation of blood flow pattern and transportation of magnetic nanoparticles in capillaries*, Intell. Technol. Appl., 2020, 1198, 222–236.

[3] AMINDARI A., KIRKKÖPRÜ K., SALTIK İL., SÜNBÜLOĞLU E., *Effect of non-linear leaflet material properties on aortic valve dynamics – A coupled fluid-structure approach*, Eng. Solid. Mech., 2021, 9 (2), 123–136.

[4] AMINDARI A., SALTIK L., KIRKKOPRU K., YACOUB M., YALCIN H.C., *Assessment of calcified aortic valve leaflet deformations and blood flow dynamics using fluid-structure interaction modeling*, Inform. Med. Unlocked, 2017, 9, 191–199.

[5] BAILOOR S., SEO J.-H., DASI L., SCHENA S., MITTAL R., *A computational study of the hemodynamics of bioprosthetic aortic valves with reduced leaflet motion*, J. Biomech., 2021, 120 (21), 110350.

[6] BELKHIRI K., BOUMEDDANE B., *A Cartesian grid generation technique for 2-D non-Newtonian blood flow through a bileaflet mechanical heart valve*, Int. J. Comput. Methods Eng., 2021, 22 (4), 297–315.

[7] BRUECKER C., LI Q., *Possible early generation of physiological helical flow could benefit the triflo trileaflet heart valve prosthesis compared to bileaflet valves*, Bioeng., 2020, 7 (4), 1–16.

[8] CARREL T., DEMBITSKY W.P., DE MOL B., OBRIST D., DREYFUS G., MEURIS B., VENNEMANN B., LAPEYRE D., SCHAFF H., *Non-physiologic closing of bi-leaflet mechanical heart prostheses requires a new tri-leaflet valve design*, Int. J. Cardiol., 2020, 304, 125–127.

[9] CLAIBORNE T.E., XENOS M., SHERIFF J., CHIU W-C., SOARES J., ALEMU Y., GUPTA S., JUDEX S., SLEPIAN M.J., BLUESTEIN D., *Towards optimization of a novel trileaflet polymeric prosthetic heart valve via device thrombogenicity emulation (DTE)*, ASAIO, 2013, 59 (3), 275–283.

[10] DIJKMAN P.E., FIORETTA E.S., FRESE L., PASQUALINI F.S., HOERSTRUP S.P., *Heart valve replacements with regenerative capacity*, Transfus. Med. Hemoth., 2016, 43 (4), 282–290.

[11] FRIES R., GRAETER T., AICHER D., REUL H., SCHMITZ C., BÖHM M., SCHÄFERS H.J., *In vitro comparison of aortic valve movement after valve-preserving aortic replacement*, J. Thorac. Cardiovasc. Surg., 2006, 132 (1), 32–37.

[12] GE L., DASI L.P., SOTIROPOULOS F., YOGANATHAN A.P., *Characterization of hemodynamic forces induced by mechanical heart valves: Reynolds vs. Viscous Stresses*, Ann. Biomed. Eng., 2008, 36 (2), 276–297.

[13] GILMANOV A., SOTIROPOULOS F., *Comparative hemodynamics in an aorta with bicuspid and trileaflet valves*, Theor. Comput. Fluid Dyn., 2016, 30, 67–85.

[14] HANAFIZADEH P., MIRKHANI N., DAVOUDI M.R., MASOUMINIA M., SADEGHY K., *Non-Newtonian blood flow simulation of diastolic phase in bileaflet mechanical heart valve implanted in a realistic aortic root containing coronary arteries*, Artif. Organs, 2016, 40 (10), E179–E191.

[15] HUI S., MAHMOOD F., MATYAL R., *Aortic valve area-technical communication: continuity and Gorlin equations revisited*, J. Cardiothorac. Vasc. Anesth., 2018, 32 (6), 2599–2606.

[16] KIM W., CHOI H., KWEON J., YANG D.H., KIM Y.-H., *Effects of pannus formation on the flow around a bileaflet mechanical heart valve*, PLoS ONE, 2020, 15 (6), e0234341.

[17] KUAN Y.H., KABINEJADIAN F., NGUYEN V.-T., SU B., YOGANATHAN A.P., LEO H.L., *Comparison of hinge microflow fields of bileaflet mechanical heart valves implanted in different sinus shape and downstream geometry*, Comput. Methods in Biomech. Biomed. Engin., 2015, 18 (16), 1785–1796.

[18] KUAN Y.H., NGUYEN V.-T., KABINEJADIAN F., LEO H.L., *Computational hemodynamic investigation of bileaflet and trileaflet mechanical heart valves*, J. Heart Valve Dis., 2015, 24 (3), 393–403.

[19] KWON Y.J., *Numerical analysis for the structural strength comparison of St. Jude Medical and Edwards MIRA bileaflet mechanical heart valve prostheses*, J. Mech. Sci. Technol., 2010, 24 (2), 461–469.

[20] LI C.-P., CHEN S.-F., LO C.-W., LU P.-C., *Turbulence characteristics downstream of a new trileaflet mechanical heart valve*, Biomed. Eng., 2011, 57 (3), 188–196.

[21] MAO W., CABALLERO A., MCKAY R., PRIMIANO C., SUN W., *Fully-coupled fluid-structure interaction simulation of the aortic and mitral valves in a realistic 3D left ventricle model*, PLoS ONE, 2017, 12 (9), e0184729.

[22] MAZZITELLI R., BOYLE F., MURPHY E., RENZULLI A., FRAGOMENI G., *Numerical prediction of the effect of aortic Left Ventricular Assist Device outflow-graft anastomosis location*, Biocybern. Biomed. Eng., 2016, 36 (2), 327–343.

[23] NASIF M.S., KADHIM S.K., AL-KAYIEM H.H., AL-WAKED R., *Using one way fluid structure interaction coupling to investigate the effect of blood flow on the bileaflet mechanical heart valve structure*, ARPN J. Eng. Appl. Sci., 2016, 11 (20), 11971–11974.

[24] PIATTI F., STURLA F., MAROM G., SHERIFF J., CLAIBORNE T.E., SLEPIAN M.J., REDAELLI A., BLUESTEIN D., *Hemodynamic and thrombogenic analysis of a trileaflet polymeric valve using a fluid–structure interaction approach*, J. Biomech., 2015, 48 (13), 3641–3649.

[25] QIAN J.-Y., GAO Z.-X., LI W.-Q., JIN Z.-J., *Cavitation suppression of bileaflet mechanical heart valves*, Cardiovasc. Eng. Technol., 2020, 11, 783–794.

[26] SAMPAIO RODRIGUES L.T., SILVA L.C., MACHADO L.C., GRECO M., GELAPE C.L., *Simulations of artificial biological heart valves with ANSYS*, Esss Comput. Model. Chall., 2016, 10.13140/RG.2.1.3146.7925.

[27] SARI M., BAYRAM Z., AYTURK M., BAYAM E., KALKAN S., GUNER A., KALCIK M., GURSOY M.O., GUNDUZ S., OZKAN M., *Characteristic localization patterns of thrombus on various brands of bileaflet mitral mechanical heart valves as assessed by three-dimensional transesophageal echocardiography and their relationship with thromboembolism*, Int. J. Card. Imaging, 2021, 37 (9), 2691–2705.

[28] SCHALLER T., SCHARFSCHWERDT M., SCHUBERT K., PRINZ C., LEMBKE U., SIEVERS H.-H., *Aortic valve replacement in sheep with a novel trileaflet mechanical heart valve prosthesis without anticoagulation*, J. Thorac. Cardiovasc. Surg., 2021, 7, 76-88.

[29] SHIBESHI S.S., VOLLINS W.E., *The rheology of blood flow in a branched arterial system*, Appl. Rheol., 2005, 15 (6), 398–405.

[30] SIEVERS H.H., SCHUBERT K., JAMALI A., SCHARFSCHWERDT M., *The influence of different inflow configurations on computational fluid dynamics in a novel three-leaflet mechanical heart valve prosthesis*, Interact. Cardiovasc. Thorac. Surg., 2018, 27 (4), 475–480.

[31] SMADI O., HASSAN I., PIBAROT P., KADEM L., *Numerical and experimental investigations of pulsatile blood flow pattern through a dysfunctional mechanical heart valve*, J. Biomech., 2010, 43 (8), 1565–1572.

[32] SUNDSTRÖM E., JONNAGIRI R., GUTMARK-LITTLE I., GUTMARK E., CRITSER P., TAYLOR M.D., TRETTER J.T., *Hemodynamics and tissue biomechanics of the thoracic aorta with a trileaflet aortic valve at different phases of valve opening*, Int. J. Numer. Method. Biomed. Eng., 2020, 36 (7), 1–14.

[33] TYFA Z., OBIDOWSKI D., REOROWICZ P., STEFAŃCZYK L., FORTUNIAK J., JÓŹWIK K., *Numerical simulations of the pulsatile blood flow in the different types of arterial fenestrations: Comparable analysis of multiple vascular geometries*, Biocybern. Biomed. Eng., 2018, 38 (2), 228–242.

[34] XU X., LIU T., LI C., ZHU L., LI S., *A numerical analysis of pressure pulsation characteristics induced by unsteady blood flow in a bileaflet mechanical heart valve*, Processes, 2019, 7 (4), 232.

[35] YUN B.M., WU J., SIMON H.A., ARJUNON S., SOTIROPOULOS F., AIDUN C.K., YOGANATHAN A.P., *A numerical investigation of blood damage in the hinge area of aortic bileaflet mechanical heart valves during the leakage phase*, Ann. Biomed. Eng., 2012, 40 (7), 1468–1485.